Nonlinear Tracking Control for Satellite Formations

Hsi-Han Yeh, Eric Nelson, and Andrew Sparks
Air Force Research Laboratory, AFRL/VACA, Wright Patterson AFB, OH 45433-7521

Abstract

A tracking control law using a sliding mode framework is derived to control a satellite formation. Hill's relative motion equations are used to model the follower satellite's motion relative to the leader. To minimize fuel required to maintain the formation, each satellite is constrained to reside near a natural orbit. Control forces are applied only to maintain the desired relative motion by correcting for initial offsets and perturbation effects that tend to disperse the formation. The control law is modified to account for the discontinuous nature of the control forces available with the satellite propulsive thrusters. Numerical simulations using a high-fidelity, nonlinear model demonstrate the control law performance for the full nonlinear dynamics with high order perturbations.

1 Introduction

Satellite formations are subject to different constraints than ground or air vehicle formations. Due to fuel capacity limitations, each satellite in a formation must reside near a natural orbit. Fuel is expended only to correct the initial deployment inaccuracy and to overcome the perturbation effects that tend to dislodge the satellite from the desired orbit. These perturbations include the effects of earth oblateness, atmospheric drag, and solar and lunar gravity. Among these perturbations, the most significant is the second spherical harmonic in the Earth's gravity field due to oblateness, known as the J_2 effect, which causes an uncontrolled formation to disperse [7].

This paper shows a tracking control design that forms the desired satellite formation after the initial deployment and nudges the members back into formation when they drift from the desired dynamics. Hill's (or Clohessy-Wiltshire) equations are used to model the follower satellite relative motion with respect to the leader. In Hill's equations and the complete nonlinear dynamical equations, the control variables are uniquely determined by a given output set. In mathematical language, the input and output manifolds are diffeomorphic. Thus, the tracking control guarantees system stability.

2 Sliding Mode Control

This section considers the theoretical basis for incorporating a multiple satellite formation control problem into the sliding mode framework. Consider a nonlinear dynamical system of the form

$$\begin{aligned} \dot{x}(0) &= f(x,t) + G(x,t)u(t), \\ y(t) &= h(x,t), \end{aligned} \tag{2-1}$$

where $x(t)$, $u(t)$, and $y(t)$ are n, m, and m dimensional real function vectors, $f(x,t)$, $G(x,t)$, and $h(x,t)$ are analytic vector or matrix functions of the variables x and t. For a multi-input, multi-output system, the relative degree vector $\alpha \in \mathbb{R}^m$ provides insight to sliding plane selection in a sliding mode control design. Let

$$y^{(\alpha)}(t) = a^*(x,t) + B^*(x,t)u(t). \tag{2-2}$$

The reference trajectory is represented by $\hat{y}(t)$, and the tracking error is defined as $e(t) = \hat{y}(t) - y(t)$.

We shall design a controller with a sliding plane

$$\begin{aligned} \sigma(e) &= e^{(\alpha-1)}(t) + K_{\alpha_M-1}e^{(\alpha-2)}(t) + \cdots \\ &\quad + K_0 e_s(t) + K_s e_{ss}(t) = 0, \end{aligned} \tag{2-3}$$

where

$$\begin{aligned} K_j &= \mathrm{diag}[k_{1j}\mu(\alpha_1 - j) \ \cdots \ k_{mj}\mu(\alpha_m - j)], \\ \mu(\alpha_i - j) &= \begin{cases} 1 & \text{if} \quad \alpha_i > j, \\ 0 & \text{if} \quad \alpha_i \le j, \end{cases} \\ \alpha_M &:= \max\{\alpha_1, \alpha_2, \cdots, \alpha_m\}, \\ K_s &= \mathrm{diag}[k_{1s} \ k_{2s} \ \cdots \ k_{ms}], \end{aligned}$$

$$e_s(t) = \int e(t)dt, \qquad e_{ss}(t) = \int e_s(t)dt,$$

and where $i = 1, 2, \cdots, m$ and $j = 0, 1, \cdots, \alpha_M - 1$.

Since the highest order derivative in (2-3) is lower than the relative degree of the plant by exactly one, the right-hand side of (2-3) does not involve the control vector $u(t)$. Instead, $\dot{\sigma}(e)$ will contain $u(t)$. This makes the sliding-mode control solution easy to obtain when a quadratic function of $\sigma(e)$ is used as the Lyapunov function. On the other hand, if the sliding plane is of equal or higher order than the relative degree, the sliding mode control solution becomes unwieldy. If the sliding plane is of lower order than the plant's relative degree by more than one, $\dot{\sigma}(e)$ will not explicitly depend on $u(t)$, and no sliding mode exists on $\sigma(e) = 0$. In this fashion, the relative degree vector dictates the sliding plane selection that is linear in the error signal.

We shall design an on-off sliding mode controller that keeps the plant state (2-1) on the sliding plane (2-3). We select a candidate Lyapunov function $V = \sigma^T(e)\sigma(e)/2$. The derivative of V is

$$\dot{V} = \sigma^T(e)\dot{\sigma}(e). \tag{2-4}$$

Differentiating (2-3) with the aid of (2-2) yields

$$\dot{\sigma}(e) = \tilde{u}(t) - B^*(x,t)u(t), \tag{2-5}$$

where

$$\begin{aligned} \tilde{u}(t) &= \hat{y}^{(\alpha)}(t) + K_{\alpha_M-1}e^{(\alpha-1)}(t) + \cdots \\ &\quad + K_0 e(t) + K_s e_s(t) - a^*(x,t). \end{aligned} \tag{2-6}$$

Substituting (2-5) into (2-4) gives

$$\begin{aligned} \dot{V} &= \sigma^T(e)(\tilde{u}(t) - B^*(x,t)u(t)), \\ &= \sigma^T(e)B^*(x,t)(B^{*-1}(x,t)\tilde{u}(t) - u(t)). \end{aligned} \tag{2-7}$$

Sliding-mode control design finds $u(t)$ such that $\sigma^T(e)\dot{\sigma}(e)$ is always negative. There are many ways to achieve this goal. One solution can take the following form

$$u(t) = B^{*-1}(x,t)\tilde{u}(t) + u_a(t), \tag{2-8}$$

with

$$u_a(t) = \begin{cases} \rho \ \mathrm{sgn}\ (B^{*T}(x,t)\sigma(e)), & \rho > 0, \quad \sigma(e) \ne 0, \\ 0, \quad \sigma(e) = 0, \end{cases} \tag{2-9}$$

where ρ is defined as a diagonal matrix

$$\rho := \text{diag}\ (\rho_1, \rho_2, \cdots, \rho_m), \tag{2-10}$$

and the vector signum function is a column of signum functions

$$\text{sgn}\ \sigma(e) = [\text{sgn}\sigma_1(e)\ \text{sgn}\sigma_2(e)\ \cdots\ \text{sgn}\sigma_m(e)]^T. \tag{2-11}$$

The control law (2-8) drives the system to the sliding plane. The control vector that sets $\dot{\sigma}(e)$ to zero is described as the equivalent control [3]. The sliding plane equivalent control (2-3) is the continuous component of (2-8) with $u_a(t) = 0$. Since this equivalent control forces the system to stay on a linear sliding plane, the equivalent control is also labeled as a feedback linearizing control. If the sliding plane (2-3) is chosen with dynamics that quickly reduce the error signal, then the closed-loop system will have good performance.

The equivalent control, as shown in (2-8), is difficult to implement for satellite control systems. Although the thruster pulse widths are adjustable, the thrust magnitudes are not. To implement a discontinuous sliding-mode control design without the continuous component, let

$$u(t) \quad = \quad \rho\ \text{sgn}\ (B^{*T}(x,t)\sigma(e)), \tag{2-12}$$

where $\rho_i > \max|B_i^{*-1}(x,t)\tilde{u}(t)|, i = 1, 2, \cdots, m$ and $B_i^{*-1}(x,t)$ is the ith row of $B^{*-1}(x,t)$. The control law in (2-12) gives an asymptotically stable closed-loop system, as shown by substituting (2-12) into (2-7)

$$\begin{aligned} \dot{V} &= \sigma^T(e)B^*(x,t)(B^{*-1}(x,t)\tilde{u}(t) - \rho\ \text{sgn}\ (B^{*T}(x,t)\sigma(e))), \\ &= \sigma^T(e)B^*(x,t)(-\tilde{\rho}(t)\ \text{sgn}\ (B^{*T}(x,t)\sigma(e))), \end{aligned} \tag{2-13}$$

where

$$\tilde{\rho}_i(t) = \begin{cases} \rho_i + B_i^{*-1}(x,t)\tilde{u}(t); & \text{if}\ \ (B_i^T(x,t)\sigma(e)) < 0, \\ \rho_i - B_i^{*-1}(x,t)\tilde{u}(t); & \text{if}\ \ (B_i^T(x,t)\sigma(e)) > 0, \end{cases} \tag{2-14}$$

for $i = 1, 2, \cdots, m$. Since ρ_i is sufficiently large, $\tilde{\rho}_i(t) > 0$. Therefore, $\dot{V}$ is always negative whenever $\sigma(e) \neq 0$. Thus, this control law drives the system to the sliding plane (2-3). The control vector magnitude ρ (2-12) is typically selected to reflect the application, and is easily adjusted to accommodate a changing control problem.

The control law of (2-12) can also drive any finite initial state to the sliding plane in finite time. To see this, we rearrange (2-13) to give

$$\begin{aligned} \dot{V} &= \sigma^T(e)B^*(x,t)(-\tilde{\rho}(t)\ \text{sgn}\ (B^{*T}(x,t)\sigma(e))), \\ &\leq -\rho'|\sigma^T(e)B^*(x,t)| \\ &\leq -\rho'' V^{\frac{1}{2}}, \end{aligned} \tag{2-15}$$

where $\rho', \rho'' > 0$. Since $V > 0$, multiplying equation (2-15) by $\frac{1}{2}V^{-\frac{1}{2}}$ produces

$$\frac{1}{2}V^{-\frac{1}{2}}\dot{V} \leq -\frac{1}{2}\rho'' < 0. \tag{2-16}$$

By integrating (2-16) from 0 to t, we find that

$$V^{\frac{1}{2}}(t) \leq V^{\frac{1}{2}}(0) - \frac{1}{2}\rho'' t. \tag{2-17}$$

The time required for the Lyapunov function to reach zero is now defined as T. Then (2-17) implies

$$T \leq \frac{2V^{\frac{1}{2}}(0)}{\rho''}. \tag{2-18}$$

Thus, the Lyapunov function reaches zero in finite time. The magnitude of discontinuous control is the design parameter that determines the reaching time.

The main drawback of the sliding-mode control method is that when an unstable high frequency plant mode is excited, the discontinuous control may exhibit a chattering phenomenon. Chattering describes rapid control signal switching between positive and negative values. The most common way to avoid chattering is to introduce a boundary layer on the sliding plane [3]. Other methods include synthesizing the control variable derivatives so that the control variables themselves do not chatter [1]. In the boundary layer approach, the discontinuous control law operates only when the system state is outside the boundary layer. Within the boundary layer, we implement a smooth transition from positive to negative, as the system state crosses the sliding plane.

The satellite control problem does not permit control force magnitude adjustments. Therefore, we cannot implement a smooth transition technique. Instead, we implement a signum function with a dead zone. Thus, (2-12) is modified as follows

$$u_i(t) = \begin{cases} \rho_i & \text{if} \quad \delta_i < B_i^{*T}(x,t)\sigma(e), \\ 0 & \text{if} \quad -\delta_i \leq B_i^{*T}(x,t)\sigma(e) \leq \delta_i, \\ -\rho_i & \text{if} \quad B_i^{*T}(x,t)\sigma(e) < -\delta_i, \end{cases} \tag{2-19}$$

$$\rho_i > \max\|B_i^{*-1}(x,t)\tilde{u}(t)\|, \quad i = 1, 2, \cdots, m,$$

for small positive values of δ_i, $i = 1, 2, \cdots, m$.

The control laws (2-8), (2-12), and (2-19) all require a double integral computation, $e_{ss}(t)$, which is not a state variable of the closed-loop system. This computational burden arises from the tracking performance consideration, which requires the sliding mode equivalent control (2-6) to have one integration. In addition to the computational burden, the double integral also introduces phase lag.

3 Satellite Control Design

In this section, we discuss the sliding plane design considerations. In addition, we present a second order design example.

3.1 Control Problem Formulation

We shall consider formation control using a linear model of the satellite relative dynamics to generate a reference trajectory. In addition, the exact nonlinear model supplies the simulation's plant dynamics. As discussed earlier, the linearized equations that describe the satellite relative motion are known as Hill's (or Clohessy-Wiltshire) equations [2]

$$\begin{aligned} \ddot{x} - 2\omega\dot{y} - 3\omega^2 x &= u_x + d_x, \\ \ddot{y} + 2\omega\dot{x} &= u_y + d_y, \\ \ddot{z} + \omega^2 z &= u_z + d_z, \end{aligned} \tag{3-1}$$

where x, y, and z are the follower satellite's positions relative to a leader satellite in a circular orbit: x is in the radial direction from the earth, y is in leader satellite's tangential velocity direction, and z completes a right-hand coordinate system. The leader satellite angular velocity, ω, around the Earth, (also known as the "mean motion"), is $\omega = \sqrt{\frac{\mu}{R^3}}$ where μ is the Earth's gravitational constant and R is the radius of the leader satellite's circular orbit. The control variables (u_x, u_y and u_z) and the disturbances (d_x, d_y and d_z) are net specific forces applied to the two-satellite system. The disturbances in (3-1) include the net effects of unmodeled dynamics, net gravitational perturbations, net atmospheric drag, net solar radiation pressure, and net third body effects.

Our control problem is to design a control system for each follower satellite within the formation that drives the satellites towards a desired trajectory relative to the formation leader. In linear approximations that yield Hill's equations, all relative motion closed paths are ellipses. The desired trajectory is a sustainable, natural, elliptic relative motion path when both satellites are free of control forces and unwanted perturbations [12]. A sustainable elliptic path maintains its relative position with respect to the leader. In explicit form, the family of sustainable elliptic paths is given by:

$$\begin{aligned} \hat{x}(t) &= r\sin(\omega t+\theta), \\ \hat{y}(t) &= 2r\cos(\omega t+\theta), \\ \hat{z}(t) &= mr\sin(\omega t+\theta)+2nr\cos(\omega t+\theta), \end{aligned} \tag{3-2}$$

where r determines the relative motion path size around the leader, θ characterizes the member satellite position on the relative motion path, and m and n describe the plane slope in which the relative motion path resides [12]. Reference trajectories are chosen from this elliptic path family, which is a subset of the force free Hills equation general solution. An arbitrary initial condition may give rise to an unsustainable path, which can not sustain a formation.

Due to fuel limitations, we cannot expect the controlled satellite transient to settle in a short order time constant. The transient response should have a time constant commensurate with the leader satellite mean motion. Therefore, we shall scale the time axis so that within each scaled time unit, the leader satellite sweeps a 1 radian arc around the Earth, regardless of the satellite altitude. We introduce a new time variable, $\tau = \omega t$. When $\tau = 1$, the leader sweeps a 1 radian arc around the Earth. Since

$$\frac{dx}{dt} = \omega\frac{dx}{d\tau}, \qquad \frac{d^2x}{dt^2} = \omega^2\frac{d^2x}{d\tau^2}, \tag{3-3}$$

Hill's equations (3-1) take the following form after the independent variable t is changed to τ:

$$\begin{aligned} \ddot{x} - 2\dot{y} - 3x &= u_x + d_x, \\ \ddot{y} + 2\dot{x} &= u_y + d_y, \\ \ddot{z} + z &= u_z + d_z. \end{aligned} \tag{3-4}$$

For convenience, we are renaming the control inputs, disturbances, and derivatives so that they are with respect to τ instead of t. Note that in (3-1) and (3-4), the control forces u_x, u_y and u_z, and disturbances d_x, d_y, and d_z are net specific forces applied to the leader-member satellite system. The word net refers to the difference between the specific forces applied to the member satellite and those applied to the leader satellite. Specific forces are applied to each unit mass of the respective satellites. Specific forces are actually accelerations. In close formations, the net disturbances are greatly reduced from the absolute amount that is exerted on the member satellite. Changing the time variable to τ for the reference trajectory (3-2) yields

$$\begin{aligned} \hat{x}(\tau) &= r\sin(\tau+\theta), \\ \hat{y}(\tau) &= 2r\cos(\tau+\theta), \\ \hat{z}(\tau) &= mr\sin(\tau+\theta)+2nr\cos(\tau+\theta). \end{aligned} \tag{3-5}$$

Equations (3-4) show that the in-plane (xy-plane) dynamics given by the Hill's equations are decoupled from the cross-track (z -axis) dynamics. For the in-plane dynamics, we design a control policy so that the plant output tracks the reference trajectory

$$\hat{y}_1(\tau) = \begin{bmatrix} \hat{x}(\tau) \\ \hat{y}(\tau) \end{bmatrix} = \begin{bmatrix} r\sin(\tau+\theta) \\ 2r\cos(\tau+\theta) \end{bmatrix}, \tag{3-6}$$

for some given values of r, q, w, m and n. Likewise, we design a cross-track control policy so that the plant output tracks the reference trajectory

$$\hat{y}_2(\tau) = \hat{z}(\tau) = mr\sin(\tau+\theta)+2nr\cos(\tau+\theta). \tag{3-7}$$

Modern satellite systems use high power jets to produce the desired control forces. The jets usually operate in a short pulse sequence. Recall our assumption that pulse magnitudes are not variable, while pulse widths are variable. Therefore, we shall use the discontinuous sliding-mode control without continuous components. We shall incorporate a sliding plane boundary layer that prevents chattering as described in equation (2-19). In this control law, we need to compute $B^{*T}(x,t)$ and $\sigma(e)$. We also need $B^{*-1}(x,t)$ and $\tilde{u}(t)$ to determine the minimum control variable magnitude.

For the linear systems model, we can separately design control laws for in-plane and cross-track dynamics. Since the disturbances are in the form of matching uncertainties, we ignore the disturbances in this design, and allow the inherent sliding mode robustness to maintain system stability. First, we shall determine the plant relative degree. Writing

$$\ddot{y}_1(\tau) = a^*_{xy}(x,\tau) + B^*_{xy}(x,\tau)(u(\tau)+d(\tau)), \tag{3-8}$$

where

$$\begin{aligned} a^*_{xy}(x,\tau) &= \begin{bmatrix} 3x+2\dot{y} \\ -2\dot{x} \end{bmatrix}, \\ B^*_{xy}(x,\tau) &= \begin{bmatrix} 1 & 0 \\ 0 & 1 \end{bmatrix}. \end{aligned} \tag{3-9}$$

we see that the in-plane dynamic relative degree is (2,2). For the cross-track dynamics, we have:

$$\ddot{z} = a^*_z(z,\tau) + B^*_z(z,\tau)(u_z+d), \tag{3-10}$$

where

$$\begin{aligned} a^*_z(z,\tau) &= -z, \\ B^*_z(z,\tau) &= 1. \end{aligned} \tag{3-11}$$

Therefore, the cross track dynamics relative degree is 2.

3.2 Effects of Disturbances and Perturbations

Sliding mode control is inherently robust. The trajectories on the sliding surface exhibit invariance in the presence of bounded unknown, matched uncertainties and disturbances [11, 5]. Matched uncertainties or disturbances reside in the range of control distribution matrix. In other words, if matched uncertainties or disturbances are known, control variables can counteract against them. In the satellite formation control problem, microsatellites are modeled as point masses. The atmospheric drag, earth gravitational perturbations, third body effects, and unmodeled dynamics all result in matched perturbations within the satellite model.

Sliding mode control is intrinsically robust against matched uncertainties. The control is always driving the system towards the sliding plane. If the disturbance d is acting in the same direction as the control u, then d reinforces u and drives the system faster towards the sliding plane. Since control magnitude does not vary, control is required for a shorter duration in this direction. The performance is actually improved. Now suppose the disturbance acts in the opposite direction as the control. The system is driven towards the sliding plane more slowly. Control is required for a longer duration to enable the system to reach the sliding plane. In this fashion, the control automatically adjusts its pulse-width. When the system is on the sliding plane, the error dynamics are determined by the sliding plane parameters.

The most significant orbital perturbation is the J_2 effect. The J_2 effect accounts for Earth oblateness and the J_3 effect accounts for the earth's polar bulge. The Hill's equations (3-1) and (3-4) do not account for the non-spherical earth effects, nor the nonlinear dynamics. The J_2 effect is nearly two orders of magnitude more pronounced than J_3. These gravity perturbations will move an uncontrolled satellite from its nominal orbit. The disturbances in our model are net specific disturbances. In close formations, the net disturbances are significantly reduced from total disturbances, but are still consequential. Sabol *et al.* [7] simulated a two-satellite formation where the J_2 effect gradually disperses the formation. Solar radiation pressure and tesseral resonance are periodic and will gradually wear out the formation, causing its members to disperse relative to each other. In tracking control, the effects of solar radiation pressure and tesseral resonance are also countered by control thrusts.

3.3 Second Order Sliding Plane Design

We choose a sliding plane in the form of (2-3). The error function rapidly approaches zero when the system state is on that plane. The sliding plane produces a proportional-plus-integral-plus-derivative equivalent control on the feedback-linearized plant. Applying the satellite system relative degrees to (2-3) yields the sliding planes for both the in-plane dynamics and the cross-track dynamics in the form

$$\sigma(e) = \frac{d}{d\tau}e(\tau) + K_1 e(\tau) + K_0 e_s(\tau). \tag{3-12}$$

We will select the two complex poles as

$$p_1 = 0.05(-1 \pm j\sqrt{3}), \tag{3-13}$$

and

$$(s - p_1)(s - p_2) = s^2 + 0.1s + 0.01. \tag{3-14}$$

Comparison of (3-12) with (3-14) gives

$$K_1 = 0.1I, \qquad K_0 = 0.01I.$$

The discontinuous sliding-mode control laws with a second-order sliding-plane are obtained by substituting (3-12) and (3-15) into (2-19)

$$u_i(\tau) = \begin{cases} \rho_i & \text{if} \quad \delta_i < \dot{e}_i(\tau) + 0.1e_i(\tau) + 0.01e_{si}(\tau), \\ 0 & \text{if} \quad -\delta_i \le \dot{e}_i(\tau) + 0.1e_i(\tau) + 0.01e_{si}(\tau) \le \delta_i, \\ -\rho_i & \text{if} \quad \dot{e}_i(\tau) + 0.1e_i(\tau) + 0.01e_{si}(\tau) < -\delta_i, \end{cases}$$

$$\rho_i > \max|\tilde{u}_i(t)|, \quad i = x, y, z,$$

where the control signmal magnitude has a lower bound that is determined by simulation. In the simulation runs discussed in Section 4, we will readjust K_1 and K_2 to search for sliding plane that require minimal fuel consumption.

4 Numerical Simulation

This section summarizes the numerical simulation of a microsatellite formation using a sliding mode framework for control. A leader satellite orbits in a low-Earth, polar orbit while a follower satellite is actively controlled. The design parameters for fuel minimization are investigated.

As described in previous sections, tracking control requires a desired dynamics model of the satellite relative motion. The sliding mode controller works to minimize the differences between the desired and actual relative motion for each of the Cartesian coordinate directions. For this current research effort, we use linear Hills equations (3-1) to provide the desired relative motion. An independent sliding mode algorithm is created for each direction. Control thrusts are therefore determined and applied independently for each direction.

To account for the discrete nature of the control thrusts, we add a nonlinear block that regulates the control thrust input. In each moving coordinate frame direction, the σ function from equation (3-12) monitors the error between desired and actual relative position, relative velocity, and integral of error position. The simulation assumes instantaneous sensing of these variables. If $|\sigma|$ is less than some defined threshold, δ_i, where $i = x, y, z$, control inputs are zero. If $|\sigma|$ exceeds δ_i, a constant control force is applied. These thrust levels are adjustable to better simulate the actual thrust magnitude for a given application.

Our simulation incorporates a high fidelity orbital propogation algorithm written by Princeton Satellite Systems for Matlab. This algorithm propagates each satellite independently in the Earth Centered Inertial (ECI) reference frame. It permits user defined levels of disturbances, such as drag, solar impacts, third body impacts from the moon's gravity, and non-spherical earth impacts. In addition, the high fidelity code accepts external force inputs, providing a convenient means to simulate control forces.

We consider the case where satellites orbit the Earth in near polar orbits. The leader satellite is in a circular orbit, while the follower's orbit has some eccentricity to produce the desired relative motion. The leader satellite's starting position has an 800 km altitude, with mean anomaly, longitude of ascending node, and argument of perigee equaling zero. The relative orbit between satellites is circular. The leader exists in the formation center, while the follower satellite attempts to maintain a 1 km radius. Thrust for formationkeeping is only applied to the follower satellite; the leader satellite orbits the Earth open loop. The simulation includes the Earth oblateness effect.

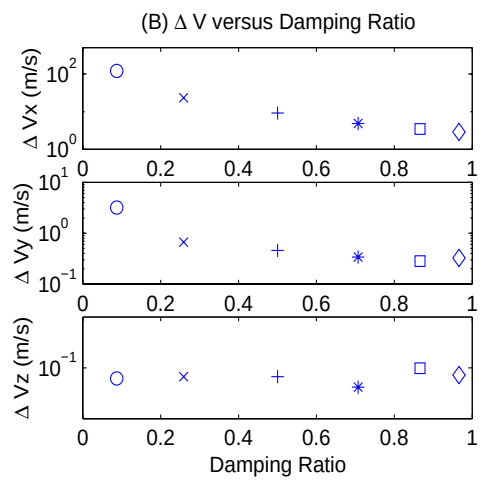

Figure 1: ΔV vs. Damping Ratio

The sliding mode design incorporates a number of design tradeoffs. In this section, all thrust levels and fuel consumptions (ΔV) are expressed in normalized "net specific values" as defined in (3-4). Note that ΔV is the integral of the specific control forces. The poles associated with the sliding surface are a primary variable when considering the closed loop design. The sliding surface gives the characteristic equation of the closed loop response when the equivalent control of the sliding mode is implemented (i.e. when the controlled system is on the sliding plane). We investigated several sliding plane pole locations to analyze their impact on fuel consumption, as measured by the amount of velocity required for stationkeeping (ΔV); see Figure 1. To formulate a reasonable com-

parison, we maintained the normalized natural frequency of the characteristic equation at 0.1. This normalized natural frequency unit results by changing the time variable from t to τ in (3-1). To minimize the ΔV requirement, the most effective cases correspond to a damping ratio between 0.866 and 0.966. These damping ratios minimize the overshoot of the thrust response. We found that the cases with smaller damping ratio less than 0.5 require additional control energy to maintain an acceptable sliding surface boundary layer (δ_i). In addition, larger damping ratios (0.966 or higher) at this natural frequency drive the follower satellite towards the desired orbit too aggressively. This overcorrection costs more energy as well.

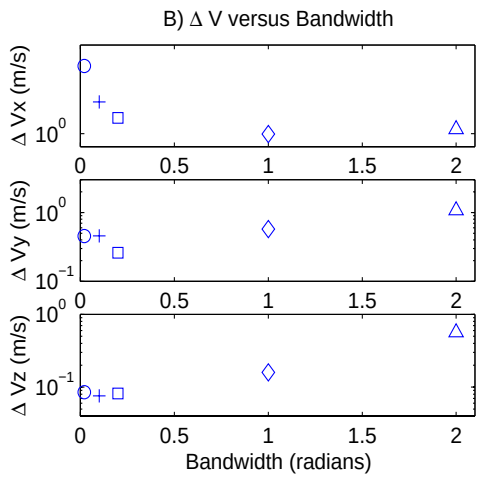

Figure 2: ΔV vs. Bandwidth

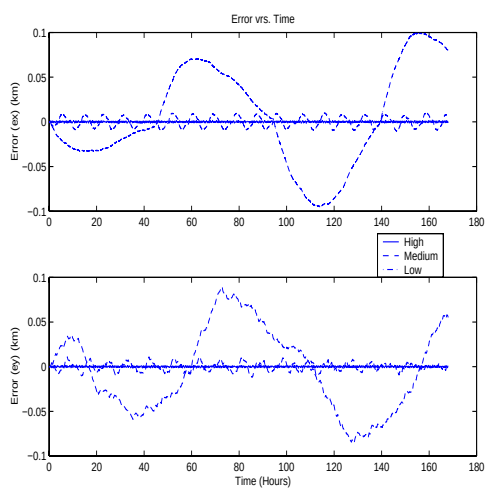

Figure 3: Response vs. Sliding Pole Bandwidth

The ΔV consumption is highly dependent on the bandwidth of the sliding plane poles. Consider the case where the characteristic pole is located along the $\zeta = 0.5$ line. For a given sliding plane boundary layer (δ_i) and corrective thrust (ρ) magnitude, some ideal bandwidth is determined. In this case, it occurs around the 1 radian bandwidth. If bandwidth is too high, the control energy tends to knock the satellite back and forth too frequently. In these cases, the disturbance forces actually cause minimal impact on the error in the satellite's relative position. See Figure 3. For this high bandwidth case (with poles represented as a $\triangle$ in Figure 2), the compensator poles are designed to cause the satellite to reach its correct position in a half revolution around the Earth (half of the 100.71 minutes for this low Earth orbit). Conversely, if the bandwidth is too low, the satellites require a long settling time. As shown in Figure 3, the satellite is "lightly" tapped to correct the orbit. The low bandwidth response can require an excessive amount of control energy over the long run. This case corresponds to the pole represented by $\bigcirc$ in Figure 2.

Another major variable that impacts the desirability of the sliding mode pole location is the thrust magnitude. Recall that the high fidelity simulation allows direct acceleration thrust insertions into the model. Figure 4 indicates the impact of thrust level for a typical medium bandwidth and moderate damping ratio (where $\zeta = 0.5$). One can achieve improved performance by increasing the corrective thrust level for a given threshold level to a point. Increasing the thrust levels beyond this point overcompensates, resulting in wasted energy from the tighter position error. The solid line on Figure 5 shows the tighter trajectory tracking. Thrust magnitude decreases also require excessive ΔV requirements and create looser positional error. This position error is shown by the dash-dot line in Figure 5.

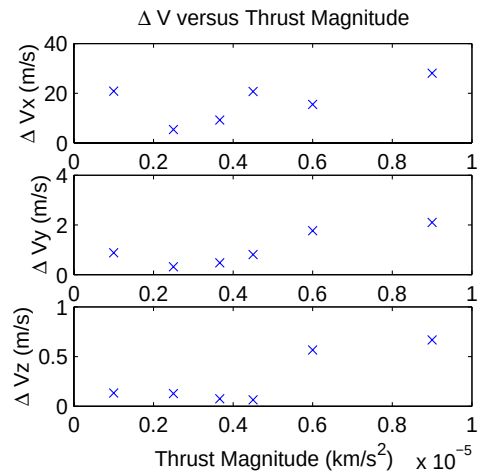

Figure 4: ΔV vs. Thrust Magnitude

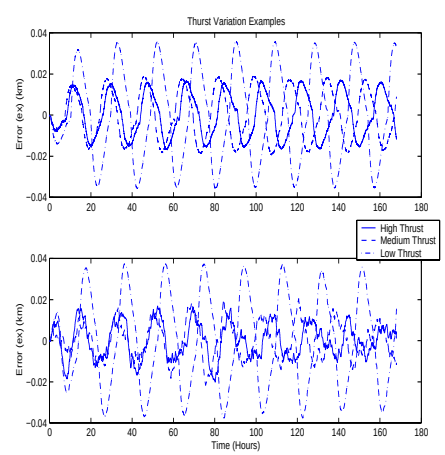

Figure 5: Response vs. Thrust Level

One can draw similar conclusions about the threshold values that trigger the corrective thrusts. Varying δ_i produces a parabolic ΔV curve (Figure 6). Given some selection for control parameters such as damping ratio and natural frequency, we can formulate some rule of thumb that relates the triggering threshold for the prescribed thrust magnitude. Excessive drift usually requires too much corrective thrust to make

loose tolerances feasible. On the other hand, excessively tight tolerances cause overcompensation, as the satellite bounces between threshold extremes.

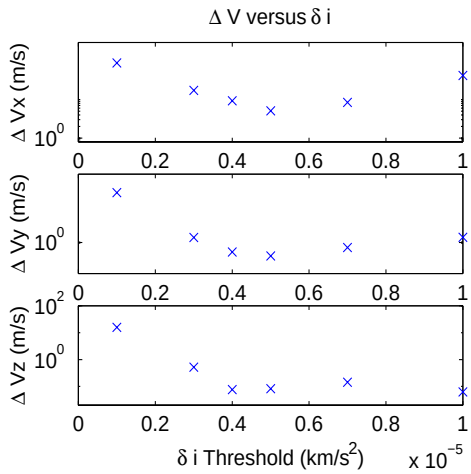

Figure 6: ΔV vs. Thrusting Threshold

The sliding mode design is robust to various perturbations. The methodology only requires a tracking signal that indicates what the desired relative position and velocity vectors are. Recall that we track a trajectory derived from the linear Hills equation as our desired dynamics. We compare two orbiting dynamic models: the high fidelity simulation with J_2 only and the all perturbative force options available in the high fidelity simulation including higher order Earth gravitational effects, atmospheric drag, solar radiation, solar disturbances, and lunar and solar gravity.

We found that as the bandwidth of the closed loop system increases, the differences in perturbative forces becomes negligible in terms of fuel usage compared to the J_2 case discussed earlier. This is because more power is used to drive the system towards the sliding mode and disturbance affects are attenuated more effectively. The disturbance effects are more noticeable at lower bandwidth designs. There are negligible closed loop response differences between the J_2 only disturbance case and numerous perturbation case. In fact, for a simulation with a one week duration, the J_2-only case requries approximately the same ΔV as the extensive perturbation case, to within 1%. Figure 7 shows the similar position error for these cases. This supports the conclusion that J_2 is the dominant perturbation at this orbit trajectory.

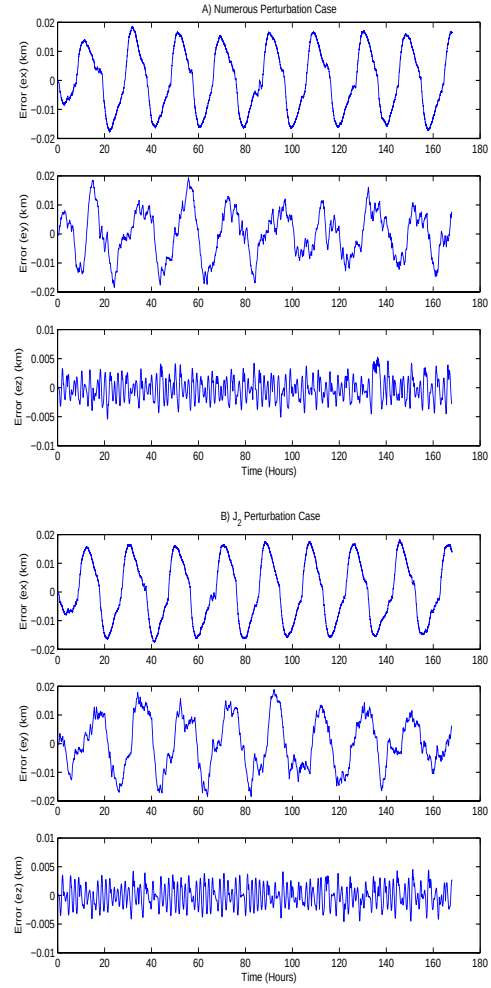

Figure 7: Responses for Nominal and Perturbed Dynamics

References

[1] Bartolini, G. and Pydynowski, P., "An Improved Chattering Free VSC Scheme for Uncertain Dynamical Systems," IEEE Transactions on Automatic Control, Vol. 41, pp 1220-246, 1998.

[2] Clohessy, W. H. and Wiltshire, R. H., "Terminal Guidance System for Satellite Rendezvous," *Journal of the Aerospace Sciences*, Vol. 27, pp 653-658, 1960.

[3] De Carlo, R. A., Zak, S. H. and Mathews, G. P., "Variable Structure Control of Nonlinear Multivariable Systems: A Tutorial," *Proceedings of the IEEE*, Vol. 76, No. 3, pp 212-232, 1988.

[4] De Queiroz, M. S., Kapila, V. and Yan Q., "Adaptive Nonlinear Control of Multiple Spacecraft Formation Flying," AIAA Conference on Guidance, Navigation and Control, Portland, Oregon, 9-11 Aug. 1999.

[5] Drazenovic, B., "The Invariant Conditions in Variable Structure Systems," Automatica, Vol. 5, pp 287-295, 1969.

[6] Kapila, V., Sparks, A. G., Buffington, J. M. and Yan, Q., "Spacecraft Formation Flying: Dynamics and Control," American Control Converence, San Diego, CA, 1999.

[7] Sabol, C., Burns, R. and McLaughlin, C., "Formation Flying Design and Evolutions," AAS/AIAA Space Flight Mechanics Meeting, February, 1999.

[8] Schaub, H. and Alfriend, K. T., "J_2 Invariant Reference Orbits for Space Craft Formations," Flight Mechanics Symposium, Goddard Space Flight Center, Greenbelt, Maryland, 18-20 May 1999.

[9] Schaub, H. Vadali, S. R., Junkins, J. L. and Alfriend, K. T., "Space Craft Formation Flying Control Using Mean Orbit Elements," Astrodynamic Conference, Ankorage, AK, 1999.

[10] Singh, S. N., " Asymptotically Decoupled Discontinuous Control of Systems and Nonlinear Aircraft Maneuver," *IEEE Transactions on Aerospace and Electronic Systems*, Vol. 25, No. 3, pp 380-390, May 1989.

[11] Slotine, J. J. and Li, W., Applied Nonlinear Control, Prentice Hall, 1991.

[12] Yeh, H. H, and Sparks, A., "Geometry and Control of Satellite Formations," American Control Conference, Chicago, IL, June 2000.